# Nanoparticle size reduction during laser ablation in aqueous solutions of cyclodextrins

J.-P. Sylvestre[a], A. V. Kabashin[a], E. Sacher[a], M. Meunier[a] and J. H. T. Luong[b]
[a]Laser Processing Laboratory, Department of Engineering Physics, Ecole Polytechnique de Montréal, Case Postale 6079, succ. Centre-Ville, Montréal, Québec, Canada, H3C 3A7
[b]Biotechnology Research Institute, National Research Council Canada, Montreal, Quebec, Canada, H4P 2R2

## ABSTRACT

The femtosecond laser ablation of gold in aqueous solution has been useded to produce colloidal gold nanoparticles. We consider the effect of size reduction through the use of aqueous cyclodextrin (α-CD, β-CD or γ-CD) solutions. Both the size reduction and the colloid stability depend on the type of CD, with the smallest, almost monodispersed and extremely stable particles prepared with β-CD, followed by slightly larger ones fabricated in γ-CD and α-CD. Several studies were carried out to elucidate the nature of the interaction between the gold and CDs. In particular, we studied the influence of pH on the size distribution and the electric charge of the gold particles surface. We examined the gold surface composition and determined the nature of the chemical groups on the gold. This enabled us to develop a model of chemical interactions between the gold and the CDs, which includes both a hydrophobic interaction of the $Au^0$ with the interior cavity of the CD and a hydrogen bonding of $-O^-$ groups, on the partially oxidized gold surface, with –OH groups of the CDs. These nanoparticles are of importance in biosensing applications.

**Keywords:** Femtosecond laser ablation in liquids, gold nanoparticles, cyclodextrins.

## 1. INTRODUCTION

Small gold nanoparticles (< 30 nm) exhibit a sharp light absorption peak at about 520 nm, due to the resonant excitation of surface plasmon oscillations[1]. When conjugated to receptors, these nanoparticles can be employed for biosensing applications, e.g., as optical markers to screen selective biointeractions[2]. For such applications, gold nanoparticles must be smaller than 30 nm and have a narrow size distribution to exhibit similar physical properties. They should also have specific chemical groups on their surfaces to link to the target biomolecule of interest. Many methods have been developed to produce small gold nanoparticles by wet chemical routes over the years[3]. Typically, a dilute metal salt is reduced in an aqueous solution containing a reducing reagent[4]. However, wet chemical methods generally lead to the production of gold particles with complex surface chemistry. For example, when gold particles are produced by citrate reduction of chloroauric acid, strongly adsorbed citrate ions modify the metal surface[2-4]. This complicates the further stabilization of the colloidal solution and the functionalization of the gold surface for biomolecule immobilization.

The laser-induced ablation of a solid target placed in a liquid environment has been used as an alternative physical method for producing metallic and semiconductive colloids[6-16]. When performed in a controllable, contamination-free environment, this method produces almost pure nanomaterials. However, laser ablation in pure water generally results in relatively large (20-300 nm), highly dispersed (50-300 nm) particles because of the post-ablation coalescence of nanoclusters[10-17]. Aqueous solutions of surfactants, which cover the particles during the condensation and thus prevent them from the further coalescence and agglomeration, have been used to drastically reduce the size of Au and Ag nanoparticles[10-12]. For example, sodium dodecyl sulfate (SDS) was used to produce Au nanoparticles with mean particle sizes as small as 5 nm[11]. However, gold nanoparticles covered with SDS could be problematical for biological applications because this molecule is known to denature biomolecules (biomolecules in the presence of SDS lose their 3D conformation).

On ablating a gold target with femtosecond radiation in surfactant-free, aqueous solutions of cyclodextrins, we recently demonstrated the formation of gold nanoparticles with a mean size of 2-2.5 nm and a size dispersion of 1-1.5 nm[17]. Cyclodextrins are torus-like macrocycles built up from glucopyranose units.[18,19] Since their interior cavity, as well as the primary face (see Fig. 1), are hydrophobic, while the secondary face and exterior surface are hydrophilic, cyclodextrins are often used in medicine and pharmacology to solubilize hydrophobic substances, such as some drugs, into aqueous solution. We used three common forms of CDs, α, β, and γ-CD, containing, respectively, 6, 7 and 8 glucopyranose units, and found that the nanoparticles produced in their presence were smaller and much more stable for β-CD, followed in order by γ-CD and α-CD. The better efficiency of β-CD in the nanofabrication experiments is thought to provide strong evidence that the mechanism of particle size reduction is related to hydrophobic interactions between the metal gold surface, which is naturally hydrophobic, and the hydrophobic cavities of the CD molecules. In this case, the formation of stable inclusion complexes of gold nanoclusters with CDs severely limits the number of free nanoclusters that are able to coalescence into larger particles. Indeed, with lower solubility (18.5 g/L) in deionized water, β-CD should exhibit the strongest hydrophobic interaction with gold, compared to both α- (145 g/L) and γ-CD (232 g/L).

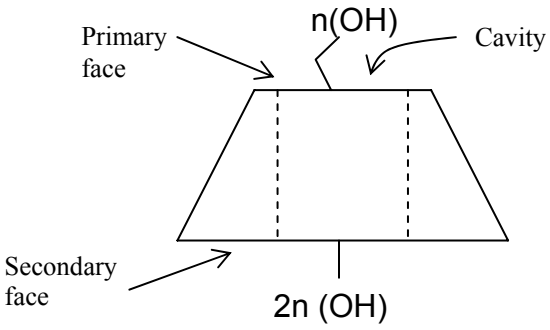


Fig. 1 Side view of a cyclodextrin molecule. For α, β, and γ-CD molecules n equals respectively 6, 7 and 8.

In this paper, we use aqueous solutions of β-CD, the most effective substance in nanoparticle size reduction, as a model to further investigate the possible mechanisms of interaction between gold particles produced by laser ablation and CD molecules. We study the effect of pH on the size distribution and charge of the nanoparticles produced and examine their chemical composition. We propose a model for the interaction between CDs and gold nanoparticles.

## 2. EXPERIMENTAL SECTION

**Femtosecond Laser Ablation.** Laser ablation was carried out with a Ti/sapphire laser (Hurricane, Spectra Physics Lasers, Mountain View, CA), which provided <120 fs full width at half maximum (FWHM) pulses (wavelength 800 nm, maximum energy 1 mJ/pulse, repetition rate of 1 kHz). The radiation was focused by an objective with the focal distance 7.5 cm onto a gold target, which was placed on the bottom of a 3-mL glass vessel filled with the desired aqueous solution (Figure 2). The laser fluence on the target surface was about 600 J/cm$^2$. The depth of the liquid layer above the gold rod (99.99%, Alfa Aesar), with diameter 6 mm and height 2 mm was 12 mm. The vessel was placed on a horizontal platform, which executed repetitive circular motions at a constant speed of 0.5 mm/s to form a circular ablated region on the target surface.

All solutions were prepared from high-purity deionized water (18 MΩ cm). NaCl (99+%, Sigma-Aldrich) solutions had pH values corrected with HCl (0.1 N solution in water, Sigma-Aldrich) or NaOH (0.1 N solution in water, Sigma-Aldrich). β-CD (Sigma-Aldrich) solutions were prepared as stock solutions in appropriate buffers immediately prior to their use.

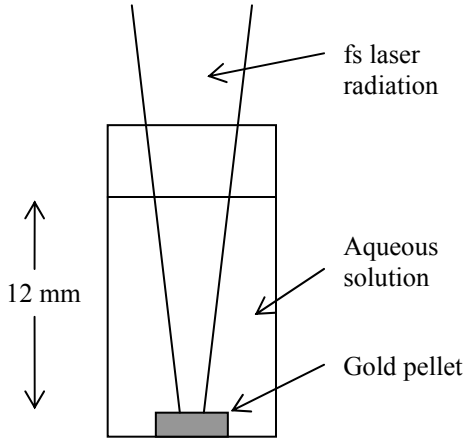


Fig. 2 Schematic representation of laser ablation in liquids.

**Measurements.** X-ray photoemission spectroscopy (XPS) analysis took place in a VG ESCALAB 3 Mark II, using a non-monochromated Mg $K_\alpha$ X-ray source at 1253.6 eV, at a base pressure below $10^{-10}$ torr. For sample preparation, drops of the colloidal solution were put on a highly oriented pyrolythic graphite (HOPG) substrate and dried overnight in a dissicator. High-resolution spectra were obtained at a perpendicular take-off angle, using a pass energy of 20 eV and 0.05 eV steps. Spectral peaks were separated using the VG Avantage program, and Shirley background removal was employed. All peaks were calibrated by setting the C1s HOPG peak to 284.5 eV. Zeta potential measurements were performed with the Zetasizer ZS (Malvern). Typically, 100 µl of the gold solution was added to 900 µl of the same solution that was used for the fabrication of the particles and the resulting diluted gold sol was injected into the analysis electrophoretic cell. A transmission electron microscope (TEM Philips CM30), with 0.23 nm point-to-point resolution, was used to take the electron images of the nanoparticles in the solution. A drop of sample solution was placed on a carbon-coated, formvar-covered copper grid, and dried at room temperature. The grid was washed with deionized water to remove unbound CD. Typically, the diameters of 500-1000 particles observed on a given micrograph were measured and the particle size (diameter) distribution was calculated.

## 3. RESULTS

### 3.1 Effect of pH on the particle distribution

To understand the mechanism of particle size reduction by CD, we studied the influence of pH of the CD solution on the laser-assisted nanofabrication process. The ablation of gold was carried out in 10mM β-CD, at pH 3, 5, 6 and 9. We observed a visible coloration of the solution after several seconds of ablation. The solution color prepared at pH > 5 was deeply red or pink, similar to Ref. 17, consistent with the presence of 3-30 nm gold nanoparticles in the solution. However, at pH < 5 the solution appeared blue-grey, suggesting that much larger particles were produced. The particles prepared at high pH values were conspicuously stable without stabilizing agent, while the nanoparticles prepared at pH 3 agglomerated within minutes, as observed by color degradation. The analysis of the size of the particles produced was obtained from TEM data, shown in Fig. 3. For high pH values (pH 6 and 9, the mean particle size was about 2.5 nm and the size dispersion did not exceed 1.5-2 nm FWHM (Fig. 3 c,d). In these cases, the mean size and dispersion were almost independent of the pH value. In contrast, particles prepared at low pH values were much larger and had much stronger size dispersions (Fig. 3a,b), suggesting that the size reduction mechanism was much less efficient at low pHs. Largest particles, of about 20 nm, were observed at pH 3. As shown in Fig. 4, there is a critical point around pH 6, in which the reduction mechanism displayed a dramatic qualitative change. In order to clarify possible reasons of this change we carried out a detailed analysis of the gold nanoparticles surface.

a) pH = 3

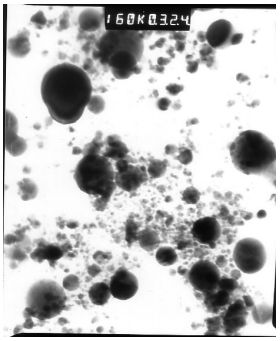

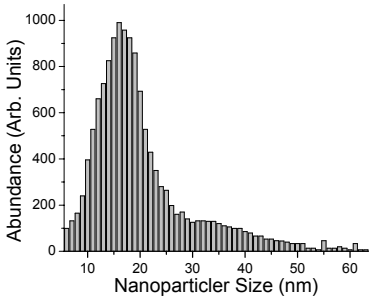


UNSTABLE

b) pH = 5

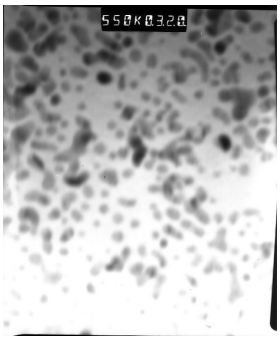

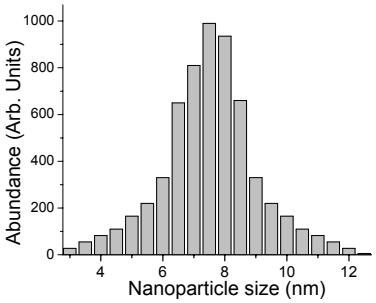


STABLE

c) pH = 6

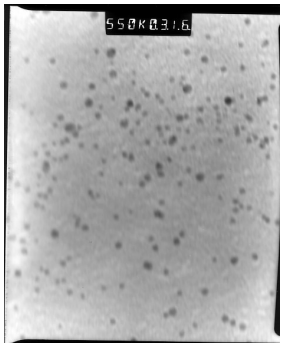

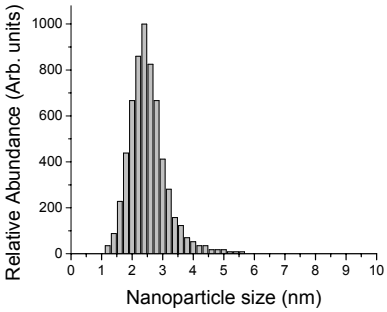


STABLE

d) pH = 9

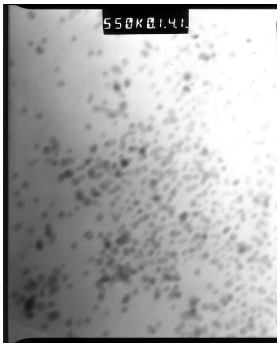

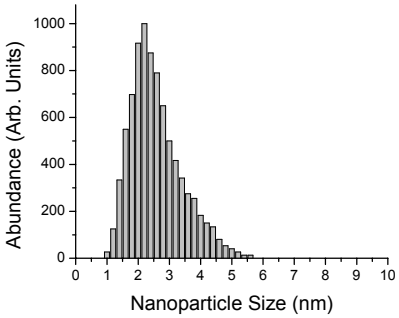


STABLE

Fig. 3 TEM pictures, size distributions and stability indication of gold nanoparticles produced in 10 mM β-CD fixed at different pH values. All other processing conditions were the same.

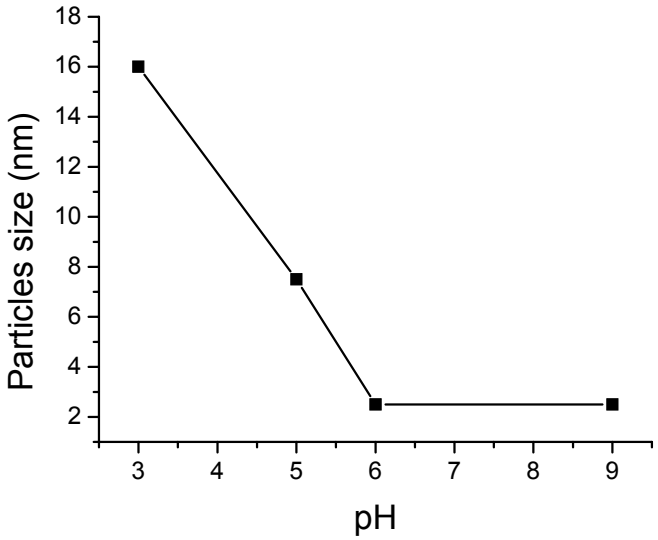


Fig. 4 Mean size of gold nanoparticles, produced in 10 mM β-CD, as a function of the pH value of the solution. All other processing conditions were the same.

### 3.2 Effect of pH on particle charging

The surface charge present on the particles in solution is of critical importance for the solution stability, as electrostatic repulsion between particles prevents their aggregation[20]. The surface charge was examined by zeta potential measurements, by recording the electrophoretic velocity of the particles when an electrical field is applied across the gold solution. Using these data, an electrical potential can be obtained. Note that the value of the measured zeta potential should slightly exceed the real surface potential, since it also depends on adsorbed ions of the opposite sign[20]. The zeta potential measurements require the use of conductive electrolytic solutions. Therefore, the tests were carried out in 10 mM NaCl electrolytic solutions, brought to different pH values. For the used pH values, variations of ionic strength did not exceed 10%.

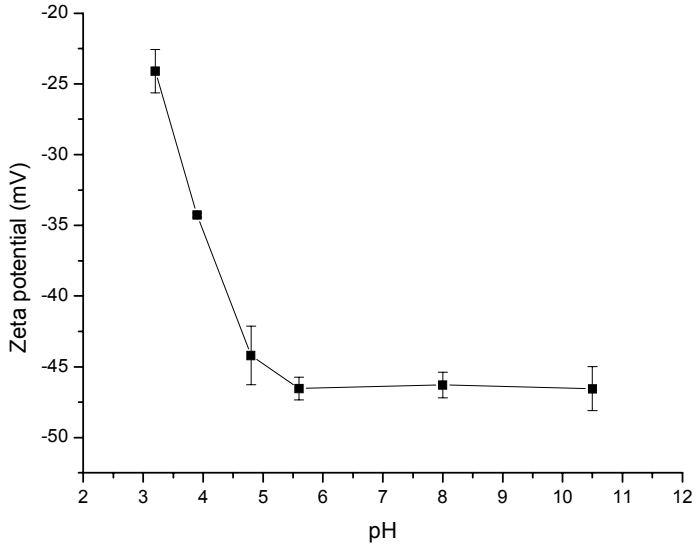


Fig. 5 Zeta potential measurements as a function of the pH of the solution used during processing.

We found that the particles produced were negatively charged for all samples. Below pH 5.8, the absolute value of zeta potential decreased as the pH decreased whereas, above pH 5.8, the absolute value of the zeta potential became almost constant, as shown in Fig. 5. In addition, the experiments at pH below 5.8 were accompanied by a much faster agglomeration of the gold sols. This process was especially strong at pH 3, for which agglomeration occurred during particle fabrication. Faster agglomeration is consistent with the measured decrease of surface charge, which leads to a reduction of the electrical repulsion between negatively charged nanoparticles.

The zeta potential data reveal the presence of a critical point (pH 5.8), very close to the point where the mean particle size drastically changes (Fig. 4). Above this point, the mean particle size was much smaller, suggesting that the efficiency of the size reduction is maximal under a relatively high negative charge of the gold surface. Such a charging effect can be explained by the presence of a chemical group able to exchange protons ($H^+$) with its surrounding environment. In the present case, an equilibrium between –OH and $–O^-$ on the gold surface, as the pH is varied, is suspected[21].

**3.3 Surface characterization of gold nanoparticles**

The surface composition of gold nanoparticles prepared in deionized water was examined by XPS. Fig. 6 shows a high resolution spectrum of the gold 4f core level. This spectrum can be characterized by three pairs of peaks, each pair due to spin-orbit coupling ($Au4f_{7/2}$ and $Au4f_{5/2}$). The analysis of the spectrum reveals partial oxidation of the gold surface. Indeed, while the first and most important pair (BEs of 84 eV and 87.3 eV) is related to elemental gold ($Au^0$), the other pairs are related to the only two stable gold oxidation states $Au^{1+}$ (BEs of 85.6 eV and 89.1 eV) and $Au^{3+}$ (BE of 87.3 eV and 90.4 eV). By comparing the relative peak areas for the three different gold compounds, we obtain their respective atomic percentages: 88.7% for $Au^0$, 6.6% for $Au^{1+}$ and 4.7% for $Au^{3+}$. In the limit of the instrument sensitivity (1%), the XPS survey scan (0-1000 eV) only reveals the presence of carbon, oxygen and gold. The presence of carbon is attributed mainly to physisorbed hydrocarbons (to lower the surface tension of the gold) and to chemisorbed bicarbonates ($HCO_3$-Au) whose presence was confirmed by FTIR and TOF-SIMS measurements (not shown here). Thus, compounds composed of gold and oxygen are suspected to be present on the surface.

The XPS technique is known to probe relatively thin near-surface layers (emerging electrons come from the first few nanometers under the surface), while inner metallic layers do not make any contribution to the integral XPS signal. Therefore, the $Au^{1+}$ and $Au^{3+}$ revealed are mainly on the surface of the particles produced. In other words, the particle surface is partially oxidized with oxygen, leading to a partially hydroxylated (Au-OH) gold surface in the presence of water. The presence of hydroxyl groups, a chemical group able to exchange protons, on the gold surface is not only consistent with the experimental data obtained with zeta potential measurements but also permits the gold particle to form its own links with the CDs via hydrogen bonding. However, XPS data are not in contradiction with our original hypothesis on the possibility of a hydrophobic interaction of the CD interior with the gold nanoparticles produced, leading to the minimization of the interfacial energy of the system. Basically, this type of interaction can make a contribution if the gold surface is also hydrophobic, as, e.g., in the case of the metallic gold. Indeed, as follows from our data, the gold surface is only partially oxidized and the hydrophobic interaction can occur in places where the oxide layer is absent. The conclusion of partial oxidation of the gold surface follows from low percentages of oxide-related compounds (6.6% for $Au^{1+}$ and 4.7% for $Au^{3+}$) in the surface layer composition.

## 4. DISCUSSION

Our results demonstrate that the size of nanoparticles produced by laser ablation in aqueous solutions of CDs depends on the pH. At pH higher than 6, the particles are very small, almost monodisperse and stable, as shown in Fig. 3c,d, whereas particles prepared at pH <6 are much larger and unstable. This cannot be explained uniquely by the originally proposed mechanism of hydrophobic interations between gold and the hydrophobic cavity of CD molecules[17]. Indeed, the change of pH should not strongly influence the hydrophobic interaction of gold nanoparticles with CDs, which possess only –OH groups at pH values below 12.

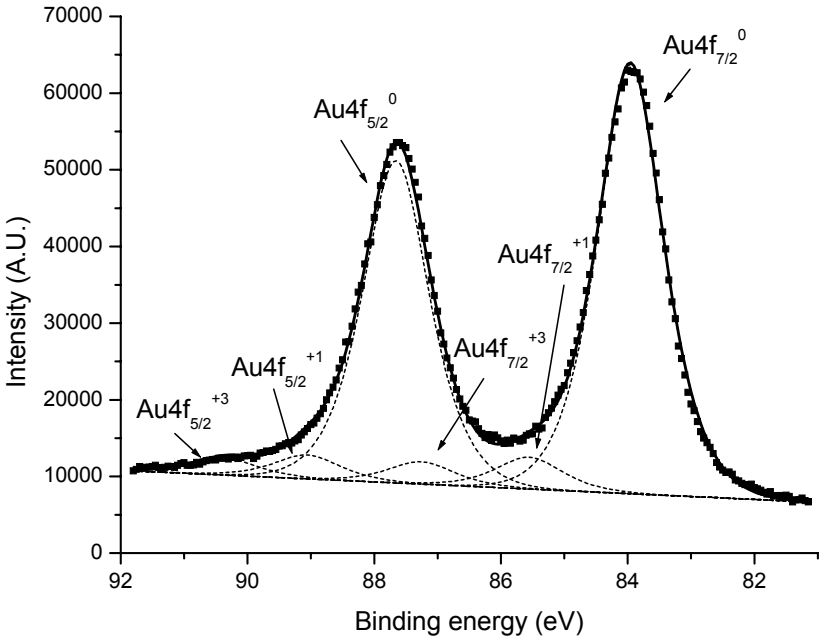


Fig. 6 X-ray photoelectron spectroscopy (XPS) spectrum of gold nanoparticles produced by laser ablation in deionized water. The dots correspond to experimental data points and the thick continuous line corresponds to the best fit, which was deconvoluted into 6 pics (short dashed curves).

Nevertheless, important information on the chemistry of gold nanoparticles obtained in this study enables us to clarify the nature of the interaction between the gold nanoparticles and CDs. Zeta potential measurements of the gold nanoparticles suggest that the nanoparticle surface is able to exchange protons with the surrounding aqueous environment. Surface characterization has confirmed that gold oxygen compounds were present on the gold surface, leading to a partially hydroxylated surface (Au-OH) in the presence of water. The negative charge at the gold surface may be explained by the fact that the Au-OH present at the surface can lose protons as the pH increases, to form Au-$O^-$ groups. It is known that hydroxyl groups (-OH) are in equilibrium with (-$O^-$) and their relative abundance is dictated by the pH value of their environment relatively to the pK value of the hydroxylated surface (pH at which the numbers of both chemical groups are equal). That is, when the pH is below the pK value, -OH groups are dominant, and when the pH is above, hydroxyl groups (-OH) loose their protons and –$O^-$ groups are dominant. In our experimental conditions, the critical point should be around pH 5 and the oxidized part of the gold surface should mainly have Au-$O^-$ groups at pH > 5 and increasing number of Au-OH groups at pH < 5. A similar model has already been used to explain the zeta potential measurements of gold thin films[21] and gold nanoparticles produced by the ultrasonic agitation, in aqueous media, of a vacuum-evaporated gold thin film[22]. The presence of –OH or –$O^-$ on the gold particles makes possible a reaction of hydrogen bonding with CDs. As shown in Fig. 1, CDs possess only –OH groups on both faces of the cavity (at pH values less than 12). It means that effective hydrogen bonding between gold and CDs is possible only when –$O^-$ groups are present on the gold surface (in contrast, the bonding is not effective when –OH groups are dominant on the gold surface because of a much weaker interaction between two –OH groups). This mechanism explains the pH dependence of the nanoparticle size. Indeed, the formation of $O^-$ takes place only at relatively high pH > 5, which corresponds to conditions of the effective reduction of gold nanoparticle size in our experiments (Fig. 4). In addition to stronger hydrogen bonding at pH > 5, the high absolute value of the surface charge of the particles fabricated in such experimental conditions could also be implicated in the production of smaller particles. Indeed, highly negatively charged nanoparticles can repeal each other more effectively, thus allowing the CD molecules to cover them before an intimate contact can occur. These kinetics considerations are believed to limit the coalescence of the forming clusters, leading to smaller particles.

Thus, a model, considering the partially hydroxylated nature of the gold surface and possible hydrogen bonding with CDs, unambiguously explains pH dependencies for the nanoparticle size and size dispersion. However, this model can not explain why β-CD is much more efficient in nanoparticle size reduction and in solution stabilization than γ-CD and α-CD. This experimental fact can only be explained by the involvement of an additional interaction between gold and CDs. As we found, the gold surface is only partially oxidized or hydroxylated. The rest of the gold surface is metallic, i.e. essentially hydrophobic. It means that some parts of the nanoparticle surface can participate in hydrophobic interactions. CDs are also known to be hydrophobic in the cavity interior and on the primary face (Fig. 1). In fact, the hydrophobicity is related to the solubility of substances in aqueous solutions. Taking into account the solubilities of different types of CDs, with 0.016 mol/L, 0.149 mol/L and 0.179 mol/L for β-CD, α-CD and γ-CD, respectively, we conclude that β-CD has a much higher hydrophobicity than α-CD and γ-CD. As a result, β-CD is capable of forming much stronger hydrophobic complexes with metallic gold, to minimize the interfacial energy of the system, in agreement with the results of our experiments[17]. The experimental results for the other types of CDs may be expained by the interplay of the two proposed mechanisms, with a much greater ability for hydrophobic interactions for β-CD (β-CD > γ-CD > α-CD) and a better ability for the hydrogen bonding reactions for CDs with a larger number of –OH groups on their primary surface (8, 7 and 6 groups for γ-CD, β-CD and α-CD, respectively).

Thus, we suggest that the reduction of nanoparticle size during laser ablation in aqueous solutions of CDs is the result of two simultaneous effects: 1) the hydrophobic interaction between the primary face of the CD molecule and inoxidized gold nanoparticle surface 2) the hydrogen bonding of the –OH groups present on the same face of the CDs and the $–O^-$ at the gold surface, as shown schematically Fig. 7. The CD molecules cover gold nanoclusters just after ablation and act like “bumpers”, limiting effectively intimate contacts between particles and thus preventing their coalescence (when the particles are still “hot”) and aggregation (when the particles are “cold”). To the best of our knowledge, it is the first time that the nature of the gold nanoparticles surface produced by laser ablation in aqueous media has been studied. We are currently continuing the analysis of the gold surface and the results will be published in due course.

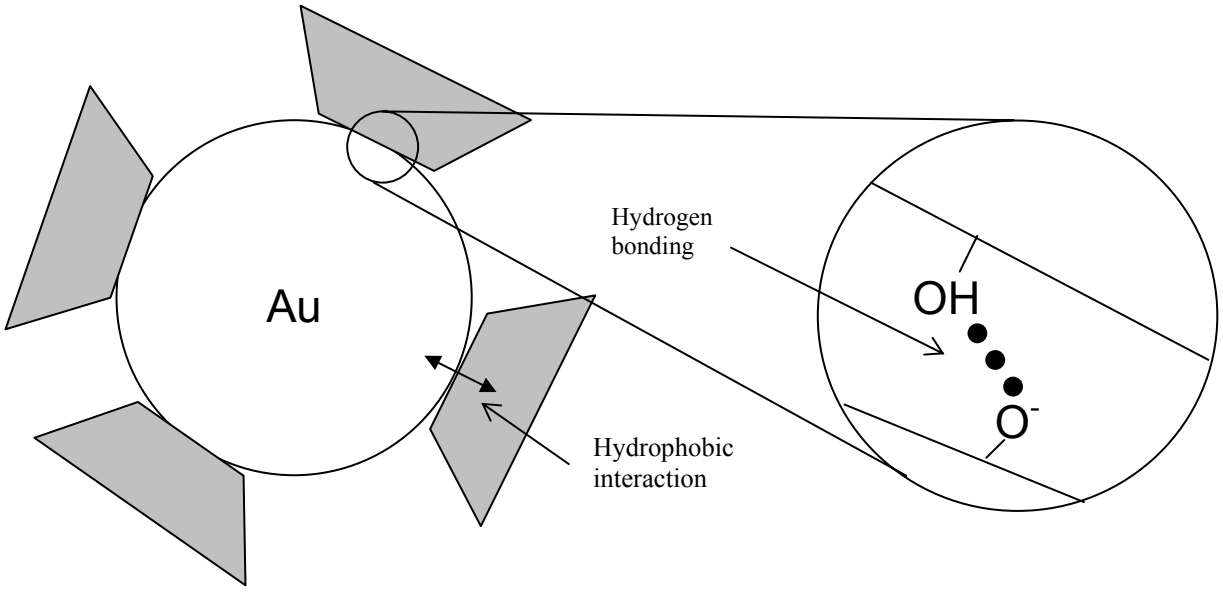


Fig. 7 The model proposed to explain the interaction between CDs and gold nanoparticles includes hydrogen bonding in addition to the hydrophobic interaction.

## 5. CONCLUSION

Femtosecond laser radiation has been used to ablate a gold target in aqueous cyclodextrin solutions to produce stable colloids of gold nanoparticles with extremely low sizes (2-2.4 nm) and dispersions (1-1.5 nm). On the basis of different chemical tests, a model of the particle growth control is proposed to explain the parameters of particles produced.

## 6. ACKNOWLEGMENTS

We thank the Natural Sciences and Engineering Research Council of Canada for funding, Dr. D.-Q. Yang (Ecole Polytechnique) for XPS measurements and Prof. J.-C. Leroux (University of Montreal) for access to the Zetasizer.

## REFERENCES

1. M. Kerker, *The scattering of light and other electromagnetic radiation* (Academic Press, New York, 1969).
2. Schultz, D.A., "Plasmon resonant particles for biological detection", Current Opinion in Biotechnology **14**, 13, 2003
3. M.-C. Daniel and D. Astruc, "Gold Nanoparticles: Assembly, Supramolecular Chemistry, Quantum-Size-Related Properties, and Applications toward Biology, Catalysis, and Nanotechnology", Chem. Rev. **104**, 293, 2004
4. M. A. Hyatt, Ed. Colloidal Gold: Principles, Methods, and Applications (Academic Press, New York, **3**, 1989).
6. A.Fojtik, and A. Henglein, *Ber. Bunsen-Ges.* Phys. Chem. **97**, 252, 1993.
7. A. Henglein, "Physicochemical Properties of Small Metal Particles in Solution: "Microelectrode" Reactions, Chemisorption, Composite Metal Particles, and the Atom-to-Metal Transition", J. Phys. Chem. **97**, 5457, 1993.
8. M. S. Sibbald, G. Chumanov, and T. M. Cotton, "Reduction of Cytochrome *c* by Halide-Modified, Laser-Ablated Silver Colloids.", J. Phys. Chem. **100**, 4672**,** 1996.
9. G. Compagnini, A. A. Scalisi and O. Puglisi, "Ablation o noble metals in liquids: a method to obtain nanoparticles in a thin polymeric film", Phys. Chem. Chem. Phys. **4**, 2787, 2002.
10. F. Mafune, J-Y. Kohno, Y. Takeda, T. Kondow, and H. Sawabe, "Formation and Size Control of Silver Nanoparticles by Laser Ablation in Aqueous Solution", J. Phys. Chem. B **104**, 9111, 2000.
11. F. Mafune, J-Y. Kohno, Y. Takeda, T. Kondow, and H. Sawabe, "Formation of Gold Nanoparticles by Laser Ablation in Aqueous Solution of Surfactant", J. Phys. Chem. B. **105**, 5114**,** 2001.
12. Y.-H. Chen, and C.-S. Yeh, "Laser ablation method: use of surfactants to form the dispersed Ag nanoparticle", Colloids & Surfaces A **197**, 133**,** 2002.
13. S. I. Dolgaev, A. V. Simakin, V. V. Voronov, G. A. Shafeev, and F. Bozon-Verduraz, "Nanoparticles produced by laser ablation of solids in liquid environment", Appl. Surf. Sci. **186**, 546, 2002.
14. T. Tsuji, K. Iryo, N. Watanabe, and M. Tsuji, "Preparation of silver nanoparticles by laser ablation in solution: influence of laser wavelength on particle size", Appl. Surf. Sci. **202**, 80, 2002.
15. T. Tsuji, T. Kakita, and M. Tsuji, "Preparation of nano-size particles of silver with femtosecond laser ablation in water", Appl. Surf. Sci. **206**, 314, 2003.
16. A. V. Kabashin and M. Meunier, "Synthesis of colloidal nanoparticles during femtosecond laser ablation of gold in water", J. Appl. Phys. **94**, 7941, 2003.
17. A. V. Kabashin, M. Meunier, K. Kingston, and J. H. T. Luong, "Fabrication and Characterization of Gold Nanoparticles by Femtosecond Laser Ablation in Aqueous Solution of Cyclodextrins", J. Phys. Chem. B **107**, 4527, 2003.
18. J.Szejtli, In *Comprehensive Supramolecular Chemistry*; J. L. Atwood, J.E.D. Davies, D.D. Macnicol, F. Vogtle, Eds. (Pergamon-Elsevier: New York, 1996; Vol. 3).
19. J.Szejtli, "Introduction and General Overview of Cyclodextrin Chemistry", Chem. Rev. **98**, 1743, 1998.
20. D.F. Evans and H. Wennerström, *The Colloidal Domain where Physics, Chemistry, Biology, and Technology Meet,* 2nd edition, Wiley-VCH, New York, 632 p. (1999)
21. J. Duval, G.K. Huijs, W.F. Throels, J. Lyklema and H.P. van Leeuwen, "Faradaic depolarization in the electrokinetics of the metal-electrolyte solution interface", Journal of Colloid and Interface Science **260**, 95, 2003.
22. D.W. Thompson and I.R. Collins, "Electrical Properties of the Gold-Aqueous Solution Interface", J. Colloid Interface Sci. **152**, pp. 197-204, 1992